Intersubband Transport in Quantum Wells in Strong Magnetic Fields Mediated by Single- and Two-Electron Scattering

K. Kempa,[1] Y. Zhou,[1] J. R. Engelbrecht,[1] P. Bakshi,[1] H. I. Ha,[1] J. Moser,[1] M. J. Naughton,[1] J. Ulrich,[2] G. Strasser,[2] E. Gornik,[2] and K. Unterrainer[2]

[1]*Department of Physics, Boston College, Chestnut Hill, Massachusetts 02467*

[2]*Institute for Solid State Electronics and Microstructure Center, Technische Universitat Wien, Austria*

(Received 4 December 2001; published 20 May 2002)

We show theoretically that in quantum wells subjected to a strong magnetic field the intersubband current peaks at magnetic field values, which reveal the underlying specific intersubband scattering mechanism. We have designed and grown a superlattice structure in which such current oscillations are clearly visible, and in which the transition from the purely single-electron to the mixed single- and two-electron scattering regimes can be observed by tuning the applied voltage bias. The measurements were conducted in ultrahigh magnetic fields (up to 45 T) to obtain the full spectrum of the current oscillations.

DOI: 10.1103/PhysRevLett.88.226803 PACS numbers: 73.63.Hs, 72.10.–d

Two-electron (electron-electron) scattering is the prime mechanism which restores the thermodynamic equilibrium in an electron gas [1]. It can play an important role in intersubband transport in quantum wells (QW) with sufficiently high carrier densities [2–5]. It was also suggested as the dominant mechanism of intersubband carrier relaxation in QW cascade structures [6] designed to emit in the THz frequency range [7]. In such structures, electron-LO phonon scattering is suppressed, since the intersubband separation is less than the LO phonon energy (~36 meV in GaAs). Other studies, however, show that *single-electron* interface roughness scattering can dominate the intersubband scattering in some QW's [8,9].

The electron-electron scattering rate $\gamma_{\text{el-el}}$ is known to be strongly dependent on the overall carrier density, its distribution over subbands, and the overlap of the relevant wave functions, i.e., the details of the structure design. For example, experiments on model QW systems show that intersubband electron-electron scattering times can be very short, of the order of 8 ps for carrier densities of 10^{11} cm^{-2}, for a strongly excited electron gas [3]. At low excitation levels (i.e., low upper subband population), however, the scattering time can be as long as 1 ns, for the same overall carrier density [2,4]. Random phase approximation (RPA) based theory fully explains these results [5]. It was recently demonstrated that applying a *magnetic field,* parallel to the growth direction of a QW structure designed as a THz emitter, improves the emission yield [10,11]. This could be understood if the magnetic field would suppress the nonradiative intersubband transport, for which electron-electron scattering is believed to be the prime candidate. Motivated by these considerations, we have examined theoretically and experimentally the influence of a strong magnetic field on the electron-electron scattering.

The details of our formalism for the electron-electron scattering in the presence of a magnetic field, applied along the growth direction of a QW, are described elsewhere [11]. We calculate $\gamma_{\text{el-el}}$ directly from the imaginary part of the electron self-energy. The screened interaction, which enters the expression for the self-energy is evaluated using RPA. We retain only the first two diagrams, since, as we have shown earlier for the $B = 0$ case, this yields essentially correct results for systems with low electron densities [5], of interest in this study. For a QW with two subbands, the final expression $\gamma_{\text{el-el}}$ of an electron from the kth Landau level of the upper subband (2) into all possible Landau levels of the lower subband (1), is [11]

$$\gamma_{\text{el-el}} = \frac{4\pi}{\hbar} \sum_{l,m,p} |V_{kl,np}|^2 \delta(E_k + E_m - E_p - E_l) \times F(m,p,l)\,, \tag{1}$$

where

$$V_{kl,np} = \iint dx\,dx' \iint dz\,dz' \phi_2^*(z)\phi_2(z')\phi_1(z)\phi_1^*(z') u_k(x - x(\beta_k)) u_l(x' - x(\beta_l)) u_m(x - x(\beta_m)) u_p(x' - x(\beta_p)) \times 2e^2 K_0[(\beta_k - \beta_m)\sqrt{(x - x')^2 + (z - z')^2}\,]\delta(\beta_k + \beta_m - \beta_p - \beta_l)\,, \tag{2}$$

and where the occupation factor is

$$F(m,p,l) = n_F(E_m)[1 - n_F(E_p)][1 - n_F(E_l)] - [1 - n_F(E_m)] n_F(E_p) n_F(E_l)\,, \tag{3}$$

where $x(\beta) = \beta/\alpha^2$, with $\alpha = \sqrt{eB/\hbar c}$, ϕ_j are the quantum well wave functions, K_0 is the modified Bessel function, and u_p are the standard harmonic oscillator wave functions of argument αx. The energies are $E_p = (p + 1/2)\hbar\omega_c + \epsilon_p$

where $\epsilon_p = \Delta$ for p located in the upper subband, $\epsilon_p = 0$ for p located in the lower subband, and $\omega_c = eB/m^*c$ is the electron cyclotron frequency corresponding to the magnetic field B and effective mass m^*. The indices k, m are the initial and l, p are the final Landau level indices of the two scattering electrons, and Δ is the intersubband energy separation. Starting with the initial two electrons in the upper subband, and ending after the scattering with two electrons in the lower subband, the energy conservation in Eq. (1) leads to

$$\Delta = \frac{n}{2}\hbar\omega_c, \qquad n = 1, 2, 3 \ldots, \tag{4}$$

where $n = p + l - k - m$. This is the 2121 process, and the notation here means that the first electron scatters from subband 2 to subband 1 (first pair of indexes), and the same happens to the other electron (second pair of indexes). γ can be nonzero only for B values which satisfy Eq. (4). Note, that in real systems in which inelastic scattering is always present, γ is never zero, and Eq. (4) becomes a condition for peaks of γ vs B. For the single-electron scattering rate γ_{se}, the golden rule formula also has the general form of Eq. (1), but with the energy conservation allowing only for "horizontal" (elastic) single electron transitions, i.e., Eq. (4), but with n even. It is obvious from Eq. (1) that the same happens (n is even) for the 2221 electron-electron scattering. This clearly shows that the different scattering processes have their respective scattering rates nonzero (or peaked for systems with inelastic scattering) for different sets of discrete values of B. Any physical process which depends on the intersubband scattering should therefore reflect this distinction, and could be used to study a specific scattering mechanism.

This distinction could be very useful, provided that there is no hidden selection rule, originating from the matrix elements of Eq. (1), which could cause $\gamma_{\text{el-el}}$ (2121) to vanish for odd n. Close inspection of Eqs. (1)–(3), as well as detailed calculations of $\gamma_{\text{el-el}}$ for various QW's, show that there is no such selection rule. Figure 1 shows an example of the calculated $\gamma_{\text{el-el}}$ vs B, for the combined 2121 and 2221 transitions, and a QW described further below. In this numerical calculation, to simulate the effects of inelastic scattering, we replace the delta function [in Eq. (1)] with its functional representation in terms of a Lorentzian with a finite width δ. Here we take $\delta = 1$ and 2 meV. To obtain the occupation factor, we have assumed a complete population inversion between the two subbands of the QW, i.e., upper and lower subband electron densities are, respectively, $N_2 \approx 10^9$ cm^{-2} and $N_1 = 0$. The calculated curve shows, as expected, peaks with maxima at B values given by Eq. (4), for both odd and even n. There is a monotonic reduction of the peak strength with n, which reflects the decreasing density of states of Landau levels. Also, the peak-to-valley ratio increases with B, primarily due to increasing separation between the Lorentzian broadened peaks. Most importantly, there is no selection rule, i.e., *no suppression of the odd peaks*. Inserts in Fig. 1 show the Landau level arrangement for three values of $n = 1, 2, 3$. For even values of n there is a perfect alignment of Landau levels between the two subbands. For odd values of n there is a midway misalignment, i.e., the Landau levels of the upper subband fall exactly in the middle between the Landau levels of the lower subband.

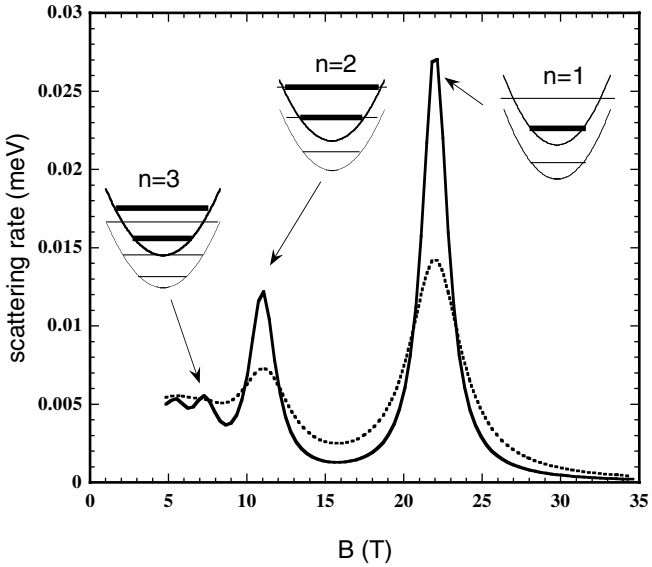

FIG. 1. Calculated electron-electron scattering rate $\gamma_{\text{el-el}}$ vs magnetic field B parallel to the growth axis, in a two-subband quantum well described in the text. Solid line assumes the Lorentzian broadening of $\delta = 1$ meV, and the dotted line $\delta = 2$ meV. Insets show corresponding, relative positions of Landau levels in the structure, for various values of B corresponding to $n = 1$, 2, and 3 in Eq. (4). Parabolas represent the energy vs momentum dispersions of the two relevant subbands for $B = 0$, and for $B \neq 0$ they serve only as a guide to the eye. Thick lines are for the upper and thin lines are for the lower subbands, respectively.

In the experimental part of this work, our goal was to design a structure in which (i) a pronounced multipeak dependence of the current density J vs B is achieved, and (ii) the transition from the purely single electron to the mixed single- and two-electron scattering regimes can be observed by tuning the applied voltage bias [12]. To have J strongly depend on the intersubband scattering, the QW must have the upper subband selectively injected, and the lower selectively extracted, and all that at nonzero bias. This requires a "chirped" superlattice as an injector/extractor. It might be tempting to use a strongly doped system to boost the electron concentration, and thereby the electron-electron scattering. However, this increased electron-electron scattering rapidly reduces population inversion in the QW, and as a result of the accordingly reduced occupation factor in Eq. (1), strongly reduces γ. In fact, we have observed such a suppression of J vs B oscillations in doped QW systems. Therefore, we choose a lightly doped system with maximized J vs B oscillations, and minimized single-electron (electron-roughness)

scattering, by improving the quality of the various interfaces which define the walls of the QW. The best design is the cascade structure described below, in which an intersubband THz emission can also be observed. In this structure, a superlattice, between each pair of QW's, selectively extracts electrons from a lower subband of the Nth quantum well, and injects them into the upper subband of the next $(N + 1)$ quantum well. Specifically [13], each segment of the cascade structure consists of the chirped superlattice sequence of thin AlAs barriers and GaAs quantum wells, with widths (in Å) 16, 148, 8, 157, 8, 178, 8, 208, 6.7, followed by the active region quantum well of width 288 Å. The two middle QW's in each chirped superlattice are doped to 10^{16} cm^{-3}. The entire structure has 49 active regions, and 50 chirped superlattices sandwiched between GaAs buffer layers of 1000 Å and Si doped to 3×10^{18} cm^{-3}. All this is grown on a 350 mm thick GaAs substrate followed by a 3000 Å buffer layer, both doped to 1.5×10^{18} cm^{-3}. The use of the high AlAs barriers eliminates undesirable cross talk between the subbands of the active region and the subbands of the chirped superlattice, thus assuring the purely two subbands scenario in each QW.

Since the intersubband scattering rate in our structure is roughly proportional to J, by measuring J we can probe the intersubband scattering. We measure J vs B for various biases, and for B in the range 0 to 45 T. The ultrahigh magnetic field is needed to observe the $n = 1$ peak. The experimental setup consists of a pulsed-magnet system with accompanying cryostat to create large pulsed magnetic fields up to 45 T in a 20 mm bore coil. This is achieved by charging a capacitor bank to a high voltage (4000 V) over a period of several minutes, and then releasing quickly (~10 msec) the stored energy (160 kJ) into a reinforced copper electromagnet, which is immersed in liquid nitrogen. Six samples were measured in all, yielding essentially identical results. We show data for a sample of area 150 mm $\times$ 100 mm. Temperature was maintained at $T = 1.9$ K. The results obtained through this setup are displayed in Fig. 2, for two biases. In addition to J vs B curves, we measured also the *THz emission* from our structure, shown in Fig. 3, using the experimental setup of Ref. [10]. From the location of the sharp peak of emission we determine the intersubband separation $\Delta \approx 19$ meV. This allowed us to confirm the validity of Eq. (4) in determining the peak positions on the J vs B curves. The inset schematically shows the Landau level arrangement $(n = 3)$ and the transition that leads to the THz emission.

Figure 2 shows J for the full range of B-field variation (0 to 45 T), for two biases $V_B = 1.7$ and 2.0 V. For biases larger than 2 V our sample enters the unstable region of domain formation (usual for cascade structures), and the J vs B curves cannot be reliably measured. As expected, positions of all observed peaks in J vs B follow Eq. (4). For $V_B = 1.7$ V, the three main peaks from the expected series of peaks are near 11 T $(n = 2)$, 6 T $(n = 4)$, and

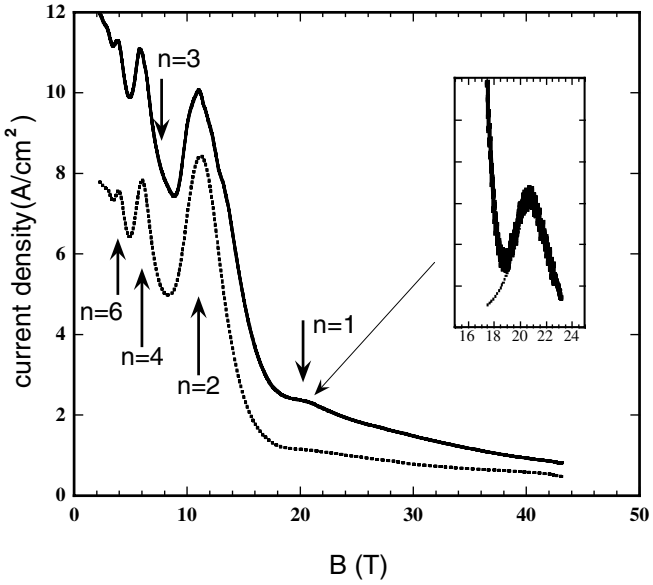

FIG. 2. Measured current density J vs magnetic field B for two biases 1.7 V (dotted) and 2 V (solid). The vertical arrows show positions of the peaks obtained from the equation (4), for the corresponding values of $n = 1$, 2, 3, 4, and 6. The inset shows a closeup of the peak, with background subtracted, at 21 T, corresponding to $n = 1$. A Lorentzian model has been fitted to this peak yielding $J_{\text{el-el}} = 0.2$ A/cm^{-2}, and $\delta = 2$ meV.

4 T $(n = 6)$. Since there are no clearly visible $n = 1$ or $n = 3$ peaks, the scattering for this bias is essentially *single electron*. For $V_B = 2.0$ V the importance of the electron-electron (two-electron) scattering increases [13], and a small but clearly visible peak develops at about 21 T, which corresponds to the $n = 1$ condition. The inset in the right upper corner makes this even clearer. It shows

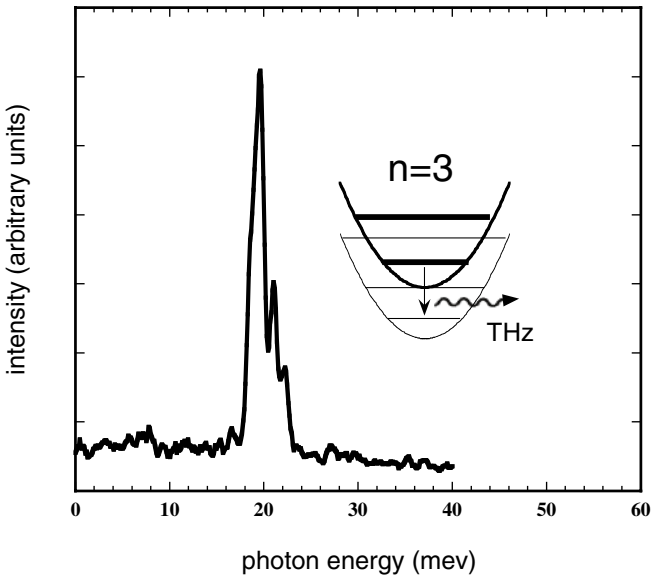

FIG. 3. Emission intensity vs emitted THz photon energy for the quantum cascade structure described in text, for $B = 0$ T. The inset schematically shows the radiative transition leading to the THz emission represented by the peak in the intensity.

the $n = 1$ peak with background subtracted, overlapping with a Lorentzian model. From this model we extract the peak strength $J_{\text{el-el}} = 0.2\ \text{A/cm}^{-2}$, and $\delta \approx 2$ meV. A careful inspection of the curve just below 8 T reveals also a presence of the tiny $n = 3$ peak.

Now, we can estimate the degree of population inversion in our structure, as defined by $p = (N_2 - N_1)/N_2$. We use here the usual flow equation $J \approx e\gamma(N_2 - N_1) = e\gamma N_2 p$ (e is the electron charge). It is valid in our low-density structure for both single- and two-electron scattering, except that, while γ_{se} is independent on N_2, $\gamma_{\text{el-el}} \sim N_2$. N_2 in the active region QW of our structure is of the order of $10^9\ \text{cm}^{-2}$. If we use $\gamma_{\text{el-el}} \approx 0.015$ meV (45 ps) from Fig. 1, $n = 1$ ($\delta = 2$ meV curve), and the extracted $n = 1$ peak strength $J_{\text{el-el}}(2V) = 0.2\ \text{A/cm}^{-2}$ (from $V_B = 2.0$ V curve), the flow equation yields p of the order of 5%, i.e., a *very weak population inversion*.

More can be obtained from the requirement of the intrawell current continuity, which gives $J = eN_1\gamma_{\text{sl}}$, where γ_{sl} is the net chirped superlattice pass through rate, essentially independent of B. Combining this with the flow equation of the previous paragraph, neglecting the small $\gamma_{\text{el-el}}$ contribution, and employing $p \ll 1$, we get $p \approx \gamma_{\text{sl}}/\gamma_{\text{se}}$. In particular this implies that p oscillates vs B (maxima of p correspond to minima of γ_{se}), and also there is a monotonic increase of peak values of p with B, reflecting the corresponding decrease of minimum values of γ_{se} with B, for large values of B. This immediately explains the observed THz emission results from a similar structure reported in Ref. [10], since the emission intensity is proportional to p. In addition, if we assume that each peak of γ (either single- or two-electron) is a Lorentzian-broadened delta function, we get that $\gamma_{\text{se}} \sim 1/B^2$, for $B \gg B$ [at $n = 2$ peak], and therefore

$$p \sim 1/\gamma_{\text{se}} \sim B^2. \tag{5}$$

For example, at $B = 42$ T we expect that $p \approx 20\%$, i.e., a much stronger population inversion. This approach might lead to the demonstration of THz lasing.

We can also estimate γ_{se} at the position of the $n = 1$ peak. Here we assume that the background current is primarily due to the tail of the $n = 2$ peak. Then, from Fig. 2 at the $n = 1$ position, we can extract separate contributions to the total J from $J_{\text{el-el}} \approx 0.2\ \text{A/cm}^2$ and $J_{\text{se}} \approx 2\ \text{A/cm}^2$, and this leads to $\gamma_{\text{el-el}}/\gamma_{\text{se}} = J_{\text{el-el}}/J_{\text{se}} \approx 0.1$, i.e., $\gamma_{\text{se}} \approx 0.15$ meV (4.5 ps). This value is consistent with the findings in Ref. [7]. From this value, in turn, we can deduce, that for $B = 0$, γ_{se} must be of the order of 1 meV ($\sim$1 ps), since the current density there is an order of magnitude larger than at $B = 21$ T. This is in agreement with the value measured [8], and shown [9] to be due to the electron-interface roughness process, for a similar QW.

In conclusion, we show theoretically that in quantum wells the intersubband current peaks at magnetic field values, which reveal the specific underlying intersubband scattering mechanism. We have shown experimentally that in a specially grown superlattice structure, which shows a sharp THz emission, such current oscillations are clearly visible. Furthermore, by tuning the applied bias, the transition from the single electron to the mixed single- and two-electron scattering regimes can be observed.

K. K. would like to thank A. Herczynski for useful comments. This work was supported in part by U.S. Army Research Office Grants No. DAAD 19-00-1-0108 and DAAD No. 19-00-1-0121, and the Austrian Science Foundation (START Y-47).

[1] S. C. Lee and I. Galbraith, Phys. Rev. B **55**, R16 025 (1997).
[2] N. Heyman, K. Unterrainer, K. Craig, B. Galdrikian, M. S. Sherwin, K. Campman, P. F. Hopkins, and A. C. Gossard, Phys. Rev. Lett. **74**, 2682 (1995).
[3] M. Hartig, S. Haacke, P. E. Selbmann, B. Deveaud, R. A. Taylor, and L. Rota, Phys. Rev. Lett. **80**, 1940 (1998); M. Hartig, J. D. Ganiere, P. E. Selbmann, S. Haacke, B. Deveaud, and L. Rota, Phys. Rev. B **60**, 1500 (1999).
[4] J. N. Heyman, J. Barnhorst, K. Unterrainer, J. Williams, M. S. Sherwin, K. Campman, and A. C. Gossard, Physica (Amsterdam) **2E**, 195 (1998).
[5] K. Kempa, P. Bakshi, J. R. Engelbrecht, and Y. Zhou, Phys. Rev. B **61**, 11 083 (2000).
[6] J. Faist, F. Capasso, C. Sirtori, D. L. Sivco, A. L. Hutchinson, M. S. Hybersten, and A. Y. Cho, Phys. Rev. Lett. **76**, 411 (1996).
[7] M. Rochat, J. Faist, M. Beck, U. Oesterle, and M. Ilegems, Appl. Phys. Lett. **73**, 3724 (1998).
[8] J. B. Williams, M. S. Shervin, K. D. Maranowski, and A. C. Gossard, Phys. Rev. Lett. **87**, 037401 (2001).
[9] C. A. Ullrich and G. Vignale, Phys. Rev. Lett. **87**, 037402 (2001).
[10] J. Ulrich, R. Zobl, K. Unterrainer, G. Strasser, and E. Gornik, Appl. Phys. Lett. **76**, 19 (2000).
[11] K. Kempa, Y. Zhou, J. R. Engelbrecht, and P. Bakshi, Phys. Rev. B (to be published).
[12] The current increases with increasing bias, and so does the population in the quantum well. This leads to an increased relative importance of the density sensitive electron-electron scattering related contribution to the total current.
[13] J. Ulrich, G. Strasser, and K. Unterrainer, Physica (Amsterdam) E (to be published).